Supplement of Hydrol. Earth Syst. Sci., 30, 6963–6981, 2026
https://doi.org/10.5194/hess-30-6963-2026-supplement
© Author(s) 2026. CC BY 4.0 License.



Hydrology and Earth System Sciences
Open Access
EGU

Supplement of

Is earlier always better? A comparative assessment of an early-stage response window for rainfall timing in multiyear drought alleviation in China

Yichen Zhang et al.

Correspondence to: Jie Zhang (zhang_jie@hainanu.edu.cn)

The copyright of individual parts of the supplement might differ from the article licence.

S1 Friedman test

Non-parametric methods such as the Friedman test (Friedman, 1937) were used in this study, as they do not require the assumption normality. The main purpose of this test is to assess whether there are significant differences in drought response (DS_{rate}) among different timings of hypothetical precipitation increases ($t_{forcing}$). The test was applied separately for each precipitation perturbations level. The null hypothesis (H_0) assumes that no significant differences exist among the four $t_{forcing}$. A p-value less than 0.05 indicates a statistically significant difference.

S2 Wilcoxon signed-rank test

Since the Friedman test only indicates whether differences exist among multiple groups, it does not provide pairwise comparisons between specific groups. Therefore, the Wilcoxon signed-rank test was applied as a post-hoc non-parametric method to evaluate pairwise differences among the $t_{forcing}$. The statistical significance of differences was assessed using p-values.

S3 Cohen's *d*

The effect size between two groups was evaluated using Cohen's *d* (Cohen, 1988). The outcome of the metric is thus the difference in group means relative to the standard deviation of the groups. In this study, the absolute value of Cohen's *d* was used to quantify the magnitude of separation. A result of 1 indicates that the group means differ by one standard deviation. Previous studies tend to use fixed thresholds to interpret small (0.2), medium (0.5), and large (0.8) effect sizes (Gevaert et al., 2018; Kratzert et al., 2019).

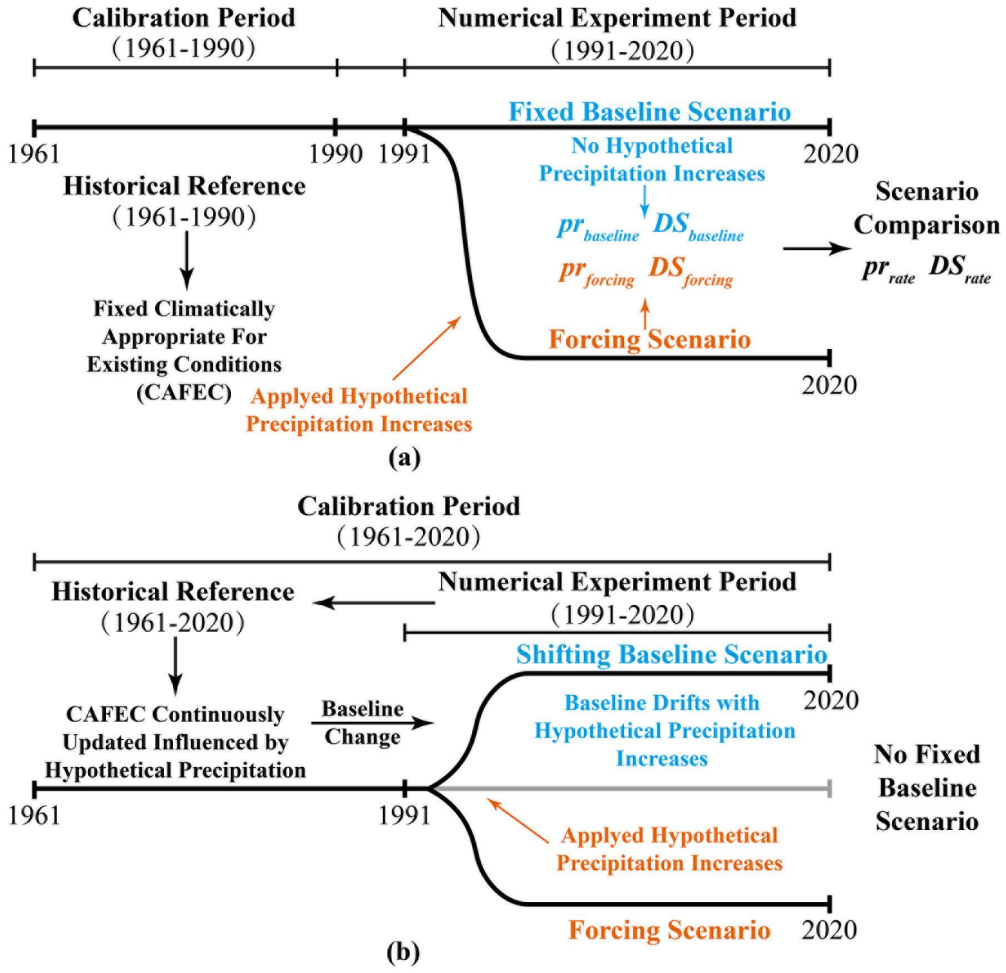
References

Cohen, J.: Statistical power analysis for the behavioral sciences, 2nd Edn., Erlbaum, Hillsdale, NJ, 1988.

Friedman, M.: The Use of Ranks to Avoid the Assumption of Normality Implicit in the Analysis of Variance, J. Am. Stat. Assoc., 32, 675–701, https://doi.org/10.1080/01621459.1937.10503522, 1937.

Gevaert, A. I., Veldkamp, T. I. E., and Ward, P. J.: The effect of climate type on timescales of drought propagation in an ensemble of global hydrological models, Hydrol. Earth Syst. Sci., 22, 4649–4665, https://doi.org/10.5194/hess-22-4649-2018, 2018.

Kratzert, F., Klotz, D., Shalev, G., Klambauer, G., Hochreiter, S., and Nearing, G.: Towards learning universal, regional, and local hydrological behaviors via machine learning applied to large-sample datasets, Hydrol. Earth Syst. Sci., 23, 5089–5110, https://doi.org/10.5194/hess-23-5089-2019, 2019.



30 **Figure S1: Conceptual illustration of the experimental design. Panel (a) shows a fixed baseline derived from a constant calibration period, while panel (b) illustrates a shifting baseline that arises when the calibration is affected by hypothetical precipitation increases imposed in the numerical experiment.**

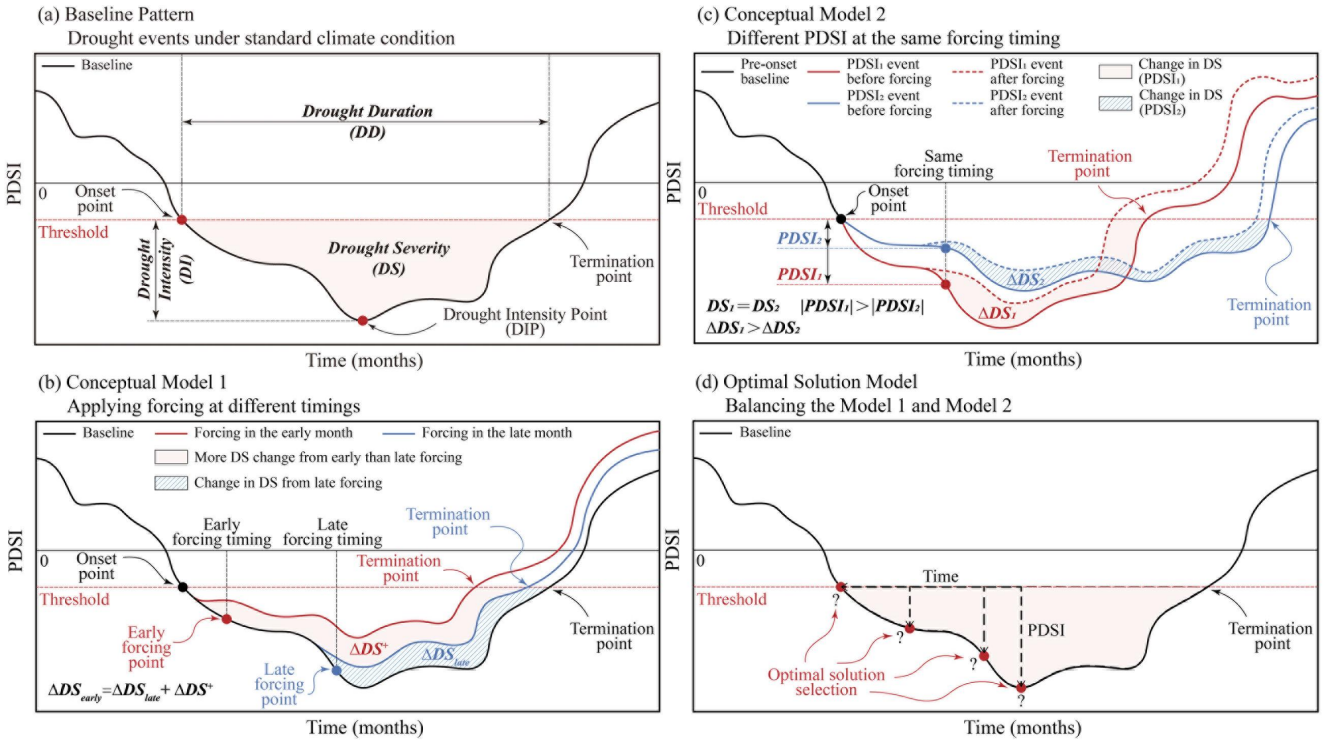


Figure S2: Conceptual models illustrating MYD alleviation driven by hypothetical increased precipitation forcing: (a) Baseline pattern without increased forcing. *DS* is represented by the area of the red region. (b) Conceptual model 1: The same hypothetical precipitation increase applied at different $t_{forcing}$ within an MYD event. An earlier $t_{forcing}$ leads to greater alleviation benefits (ΔDS^+, red area) and avoids additional losses from cumulative precipitation deficits. (c) Conceptual model 2: The same hypothetical precipitation increase applied at the same $t_{forcing}$, but with different drought index values. Because standardized drought indices exhibit tail sensitivity, deeper drought conditions tend to produce large DS reductions under identical forcing ($\Delta DS_1 > \Delta DS_2$). (d) Optimal solution model: By weighing the mismatch influences of hypothetical precipitation forcing described in Conceptual models 1 and 2, $t_{optimal}$ (marked by the red point) can be identified.

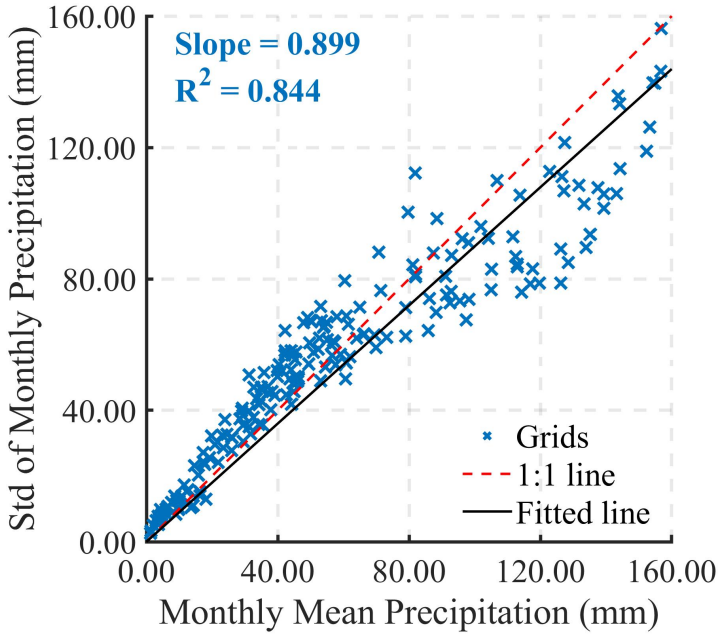


Figure S3: Relationship between mean and standard deviation of monthly precipitation across 199 grids. The red dashed line is the 1:1 line. The black solid line is the fitted line based on values from 199 grids. Blue crosses are the values for individual grids.

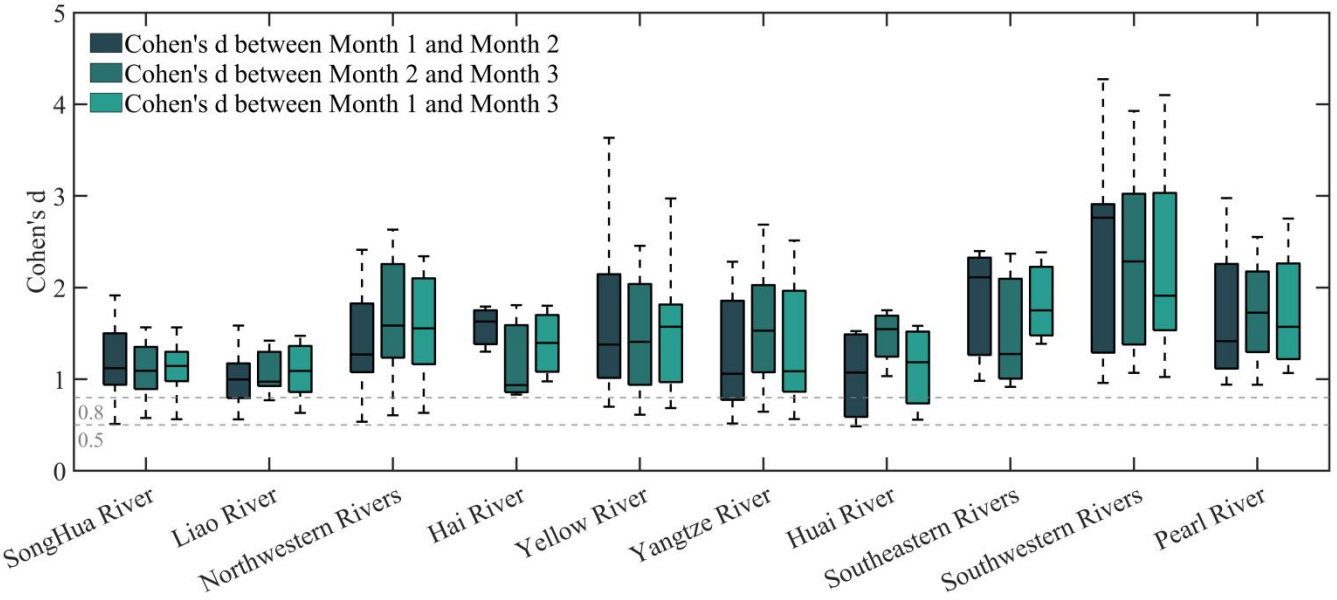


Figure S4: Basin-scale Cohen's d values for pairwise comparisons among early MYD forcing timings (t_1~t_3) across 10 major basins in China.

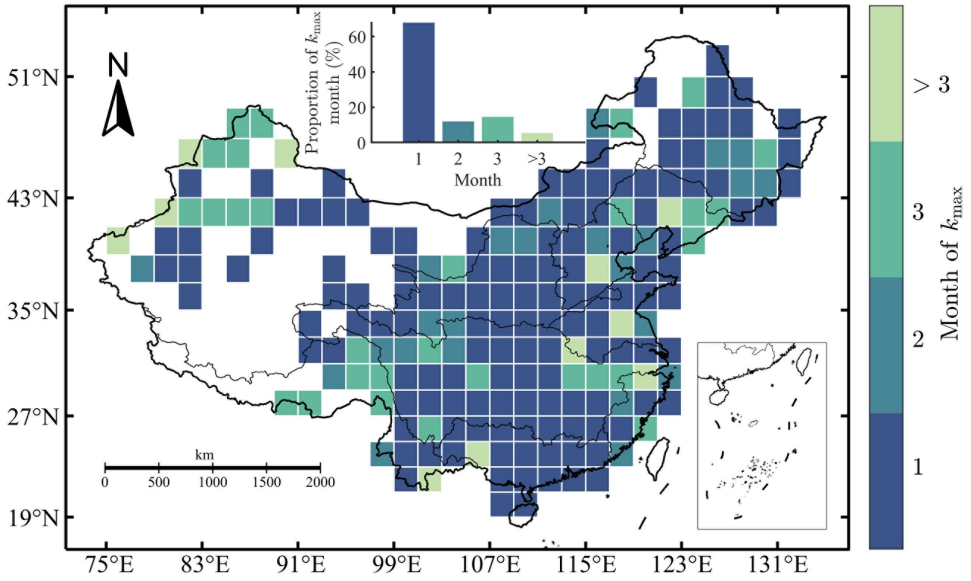


Figure. S5: Spatial distribution of the mode-based $t_{optimal}$ for each grid. For each hypothetical precipitation perturbation scenario (pr_{rate}= 0.05, 0.10, ..., 1.00), the corresponding optimal timing was first identified according to the maximum DS_{rate} among different $t_{forcing}$. Scenario without additional precipitation input (pr_{rate}= 0) was not included because identical DS_{rate} across all $t_{forcing}$ prevent a unique $t_{optimal}$ from being identified. The mode of the resulting 20 optimal timing was then used to represent the $t_{optimal}$ across different precipitation perturbation magnitudes (mode-based approach). The inset shows the frequency histogram of $t_{optimal}$ for these grids.

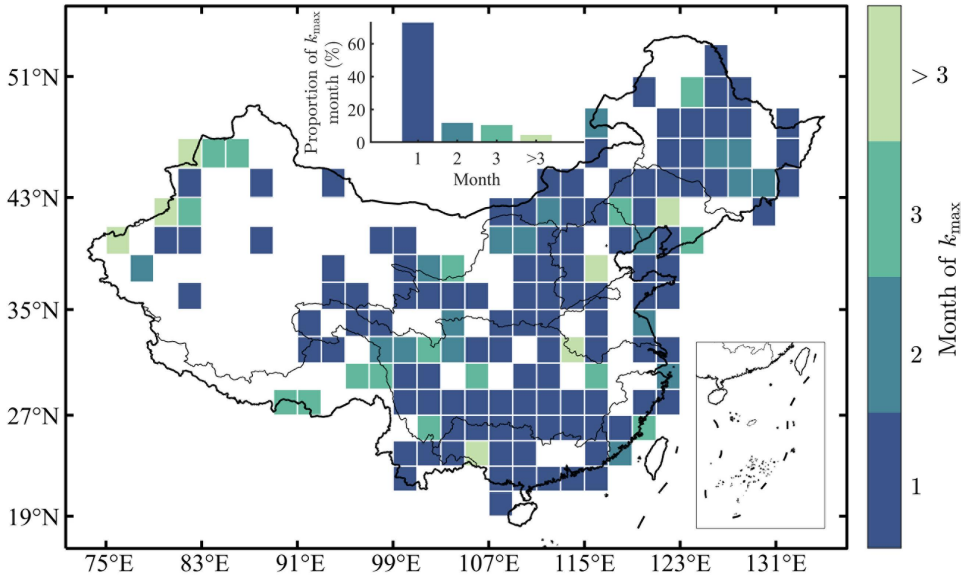


Figure. S6: Spatial distribution of the $t_{optimal}$ for grids where the mode-based and DAQM-derived $t_{optimal}$ are identical. The inset shows the frequency histogram of $t_{optimal}$ for these grids.

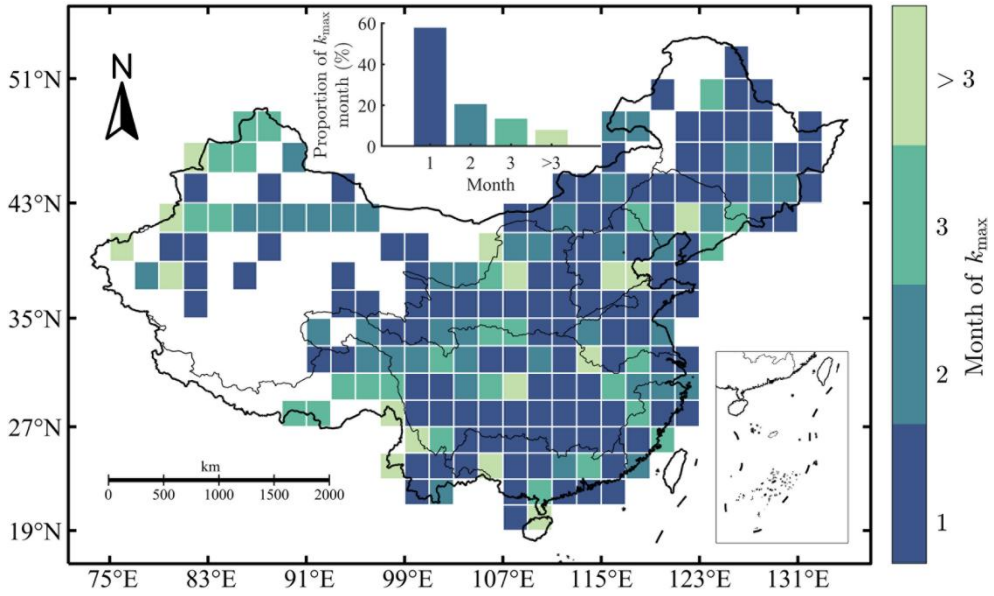


Figure. S7: Spatial distribution of the $t_{optimal}$ derived from small perturbation experiments (pr_{rate} = 0.05) for each grid. The inset shows the frequency histogram of $t_{optimal}$ for these grids.

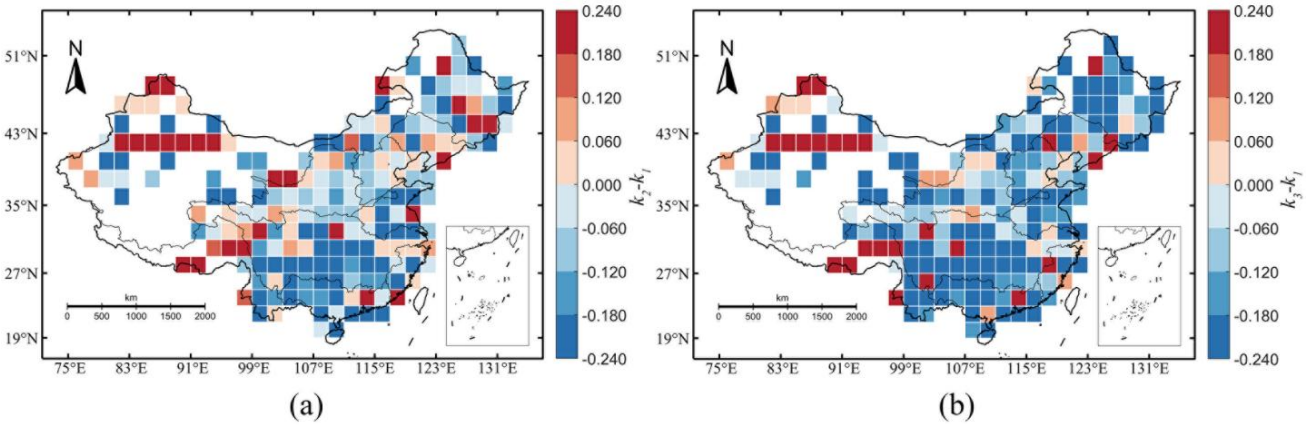


Figure. S8: Spatial distribution of the changes in k (Δk) derived from the small perturbation experiments (pr_{rate} = 0.05). (a) Change in k between t_2 and t_1 (Δk_{21}). (b) Change in k between t_3 and t_1 (Δk_{31}).

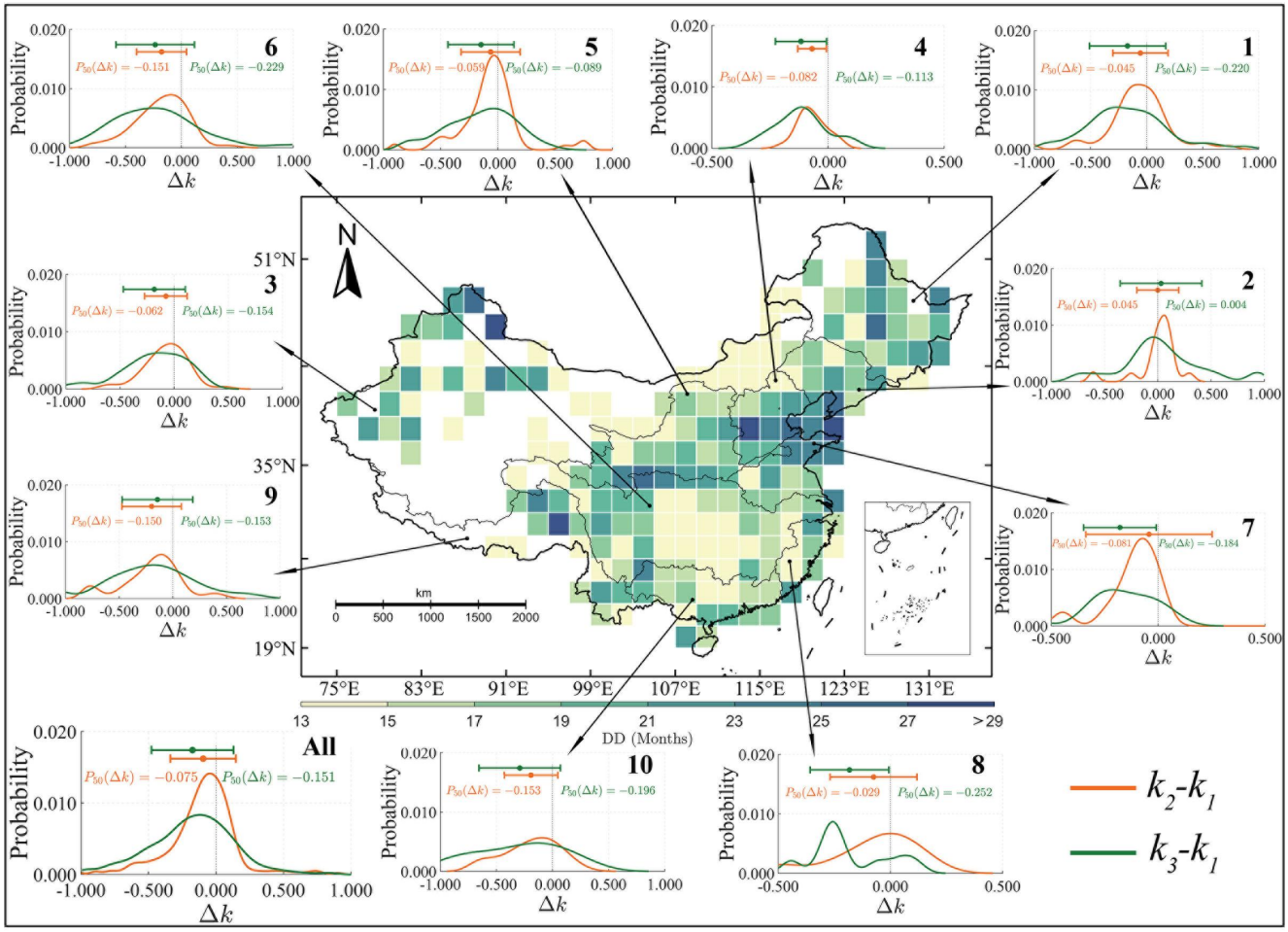


Figure. S9: Spatial distribution of the median drought duration from 1991 to 2020 across the 10 river basins in China. Surrounding panels show the probability distribution of Δk derived from the small perturbation experiments (pr_{rate} = 0.05) for all of China and each basin, based on grid-level MYD samples. Specifically, the orange lines represent Δk_{21}, and the green lines represent Δk_{31}. The *x-axis* in each panel denotes Δk, while the *y-axis* denotes probability. The number in the upper-right corner of each panel indicates the basin code.

Table S1: A list of principal symbols and acronyms

Symbols and Acronyms	Description
MYD	MultiYear Drought
PDSI	Palmer Drought Severity Index, a monthly drought index where each value represents the PDSI-defined "drought severity" for that month (the terminology is distinguished from the event-level drought severity, DS, used in this study)
DS	Drought Severity of a drought event, the cumulative deficiency of a drought index below the critical threshold throughout the event
DD	Drought Duration of a drought event, the period during which a drought index is continuously below the critical threshold during the event
DI	Drought Intensity of a drought event, the maximum deviation of the drought index below the critical threshold during the event
DDP	Drought Development Period of a drought event
DIP	DI Point of a drought event, the PDSI value corresponding to the DI
DAQM	Drought Attenuation Quantitative Model
CAFEC	Climatically Appropriate For Existing Conditions
$pr_{baseline}$	the actual precipitation in the targeted month under the baseline (no hypothetical additional precipitation is applied) scenario
$\overline{pr}$	the long-term mean monthly precipitation
$pr_{forcing}$	the precipitation in the targeted month after applying hypothetical additional precipitation
pr_{rate}	the relative change in pr, $pr_{rate}=\frac{pr_{forcing}-pr_{baseline}}{\overline{pr}}$
$DS_{baseline}$	the actual DS under the baseline (no hypothetical additional precipitation is applied) scenario
$DS_{forcing}$	the DS after the hypothetical additional precipitation is applied
DS_{rate}	the relative change in DS, $DS_{rate}=\frac{DS_{baseline}-DS_{forcing}}{DS_{baseline}}$
k	MYD attenuation efficiency, k characterizes how rapidly additional precipitation is converted into reductions in DS
$k_{theoretical}$	the theoretical k value, $k_{theoretical}$ is obtained by fitting the DAQM analytical solution $DS_{rate}=1-exp(-k\cdot pr_{rate})$ to the DS_{rate}-pr_{rate} curve derived from the numerical experiments
k_{actual}	the actual k value, represent the empirical sensitivity of DS to small precipitation perturbations, $k_{actual}=\frac{DS_{rate}(pr_{rate}=0.05)}{0.05}$, pr_{rate}=0.05 is the step size in the numerical experiments

ε	relative error, $\varepsilon=\left(\frac{k_{theoretical}-k_{actual}}{k_{actual}}\right)\times 100\%$
k_1	$k_{theoretical}$ value at the first month of a MYD event
k_2	$k_{theoretical}$ value at the second month of a MYD event
k_3	$k_{theoretical}$ value at the third month of a MYD event
k_{max}	maximum $k_{theoretical}$ within a MYD event, obtained as the largest monthly k among all months of this event
Δk_{21}	the changes in $k_{theoretical}$ between the second and the first month of a MYD event
Δk_{31}	the changes in $k_{theoretical}$ between the third and the first month of a MYD event
$t_{forcing}$	the month of hypothetical additional precipitation is applied
t_1	the first month of a MYD event
t_2	the second month of a MYD event
t_3	the third month of a MYD event
t_{DIP}	the month corresponding to DIP within a MYD event
$t_{optimal}$	the optimal timing for drought alleviation

Note: To avoid ambiguity, the monthly values of the Palmer Drought Severity Index (PDSI) are referred to simply as "PDSI" in this study, whereas DS is used exclusively to denote event-level drought severity.

Table S2: Comparison of R^2 values for different functional models

Model order	Differential form	Integral form	t_1	t_2	t_3
Zero-order	$\frac{\partial DS_{rate}}{\partial pr_{rate}}=k$	$DS_{rate}=k\cdot pr_{rate}$	0.992	0.984	0.989
First-order	$\frac{\partial DS_{rate}}{\partial pr_{rate}}=k\cdot(1-DS_{rate})$	$DS_{rate}=1-exp(-k\cdot pr_{rate})$	0.985	0.996	0.993
Second-order	$\frac{\partial DS_{rate}}{\partial pr_{rate}}=k\cdot(1-DS_{rate})^2$	$DS_{rate}=1-1/(k\cdot pr_{rate}+1)$	0.982	0.976	0.961
N-order	$\frac{\partial DS_{rate}}{\partial pr_{rate}}=k\cdot(1-DS_{rate})^n$	$DS_{rate}=1-[1-k\cdot(1-n)\cdot pr_{rate}]^{1/1-n}$	0.989	0.996	0.998

Note: t_1, t_2, and t_3 represent the first to the third month of the MultiYear Drought event.

Table S3: Pairwise statistical comparisons of DS responses among t_1-t_4 using the Friedman test, Wilcoxon signed-rank test and effect size (Cohen's d).

Comparison	p value	Effect size (Cohen's d)
t_1 vs t_2	<0.001	0.003
t_1 vs t_3	<0.001	0.003
t_2 vs t_3	<0.001	0.002
t_1 vs t_4	<0.001	0.231
t_2 vs t_4	<0.001	0.244
t_3 vs t_4	<0.001	0.342